Observed Temperature Two-Day Wave and Its Relatives near the Stratopause

VARAVUT LIMPASUVAN AND CONWAY B. LEOVY

Department of Atmospheric Sciences, University of Washington, Seattle, Washington

YVAN J. ORSOLINI

Norwegian Institute for Air Research, Kjeller, Norway

(Manuscript received 5 October 1998, in final form 22 July 1999)

ABSTRACT

The two-day wave is observed in the *Upper Atmosphere Research Satellite* Microwave Limb Sounder temperature data around 40–58 km. Between December 1991 and September 1994, the two-day wave temperature signature is most significant after each solstice when the derived easterly winds near the stratopause extend across the equator to at least 20° latitude in the winter hemisphere, and the zonal mean winds near the equator are inertially unstable with observed inertial instability disturbances. The observed two-day wave consists of a 2.0-day period zonal wavenumber-3 and a 1.8-day period zonal wavenumber-4 component, named (3, 2.0) and (4, 1.8), respectively. The (3, 2.0) component is dominant during two of the three available austral summers, but its amplitude is much weaker than the (4, 1.8) component during the two observed boreal summers.

During the austral summers, correspondence between amplification of the two-day wave temperature signatures, regions of reversed potential vorticity gradient due to meridional curvature of the zonal mean flow, and the critical lines for the (3, 2.0) and (4, 1.8) modes suggest barotropic instability as a source of both wave components. Momentum redistribution by observed inertial instability appears to barotropically destabilize the equatorward flank of the easterly jet where the wave components subsequently grow. During the boreal summers, the (4, 1.8) component appears to be excited by instability that is associated with vertical shear and curvature of the flow seated above the observational domain. The boreal (3, 2.0) mode appears unrelated to the zonal flow instability within the observational domain and may reflect a normal-mode-like response during these periods.

1. Introduction

Many interesting phenomena exist around the low-latitude stratopause region. Midlatitude, winter, quasi-stationary planetary (Rossby) waves are known to propagate meridionally into the region. Equatorially trapped Kelvin waves, originating from below, are also present. Upon nearing their critical surfaces, where their phase speed matches the zonal wind, these waves can break and irreversibly mix air constituents. The resulting mechanical and thermal damping drives residual mean circulations that govern much of the vertical and latitudinal transport in the region. In addition, mean wind acceleration by Kelvin waves, Rossby waves, and gravity waves are believed to drive meridional circulations of the semiannual oscillation (e.g., Ray et al. 1998). Other observed planetary-scale circulation features in the low-latitude stratopause region include inertially unstable disturbances (''inertial waves'') and zonal wavenumber-3 and -4 disturbances of approximately two-day period, collectively identified for historical reasons as components of the ''two-day wave.''

Inertially unstable disturbances are observed in regions where the summer easterly winds intrude into the winter hemisphere (Hitchman et al. 1987; Fritts et al. 1992; Hayashi et al. 1998). Their appearance is intimately connected with midlatitude quasi-stationary Rossby waves. As Rossby waves propagate into the low winter latitudes, they tend to draw the summer easterlies across the equator and may initiate inertial instability by meridionally displacing air parcels. The resulting vertically stacked patterns of anomaly extrema with vertical peak-to-peak scale of 5–14 km persist for about 7–14 days, and the associated circulation can mix tracers effectively (O'Sullivan and Hitchman 1992; Orsolini et al. 1997).

Two-day wave wind oscillations have long been observed in the upper mesosphere by radar reflections from meteor trails and partial radio reflections from ionospheric irregularities (e.g., Muller and Nelson 1978; Vincent 1984). However, satellite observations were the first to clearly show that the two-day wave consists of westward-propagating zonal wavenumber-3 and -4

Corresponding author address: Varavut Limpasuvan, Department of Atmospheric Sciences, University of Washington, Box 351640, Seattle, WA 98195.
E-mail: var@atmos.washington.edu

components (Rodgers and Prata 1981; Burks and Leovy 1986; Wu et al. 1996). Theoretically, the wavenumber-3 component, hereafter (3, 2.0), can arise as a Rossby normal mode that is amplified locally by the easterly zonal flow structure around the solstice (Salby 1981). The zonal wind structure can also promote modal instability of a wavenumber-3 disturbance (Plumb 1983). The wavenumber-4 component, hereafter (4, 1.8), does not correspond to a Rossby normal mode and appears to arise from instability of the zonal mean jet associated with potential vorticity gradient reversal. Norton and Thuburn (1996, 1997) successfully modeled the generation of the (4, 1.8) component and showed that vertical shear and curvature of the easterly jet generated by gravity wave drag may be responsible.

The two-day wave and inertial waves may be linked to one another, as first pointed out by Hitchman (1985). Inertial instabilities may foster favorable conditions in the easterly winds that allow barotropic instability growth of the two-day wave (Orsolini et al. 1997). Circulations associated with inertial instabilities tend to transport westerly momentum toward the summer hemisphere. In the process, the horizontal curvature of the mean wind can be significantly increased in the summer subtropics, contributing to possible modal barotropic instability through the reversal of mean potential vorticity gradient.

Alternatively, Wu et al. (1996) suggest that the (3, 2.0) component may be triggered by forcing related to the winter planetary waves. Prior to amplification of temperature two-day wave disturbances in the summer subtropics, they observed two-day wave signatures at high winter latitudes, where a broad spectrum of planetary waves is active. They suggest that such a winter wavenumber-3 two-day wave signal can radiate to the summer easterly jet core where it is greatly amplified.

This study focuses on the temperature two-day wave near the stratopause. Temperature data from the *Upper Atmosphere Research Satellite (UARS*) Microwave Limb Sounder (MLS) are used to record the wave appearance over a 3-yr period (December 1991–September 1994). Analyses of observations showing the wave structure and variability are presented. Relationships between the wave and the mean wind structure are discussed and possible mechanisms are explored.

2. Data and methods

This study uses the version 3 MLS temperature of the unbinned along-track vertical profiles (level 3AT). The MLS is one of the *UARS*'s limb viewing instruments [see Barath et al. (1993), for details]. Its latitudinal coverage alternates every 30–40 days, a consequence of the yaw-around maneuver performed by the satellite to keep some of the onboard instruments pointing directly at the sun and others away. Prior to a maneuver, the global coverage of the sounder ranges from 80° latitude in the Northern Hemisphere to 32° latitude in the Southern Hemisphere. After the maneuver, the hemispheric coverage is reversed. Regions equatorward of 32° latitude are continuously observed, while regions at higher latitudes are intermittently sampled.

For the temperature profile, independently retrieved data are given at 22, 10, 4.6, 2.2, 1.0, and 0.46 hPa. The effective MLS vertical resolution is then about 6 km. Estimations of the retrieved profile precision and accuracy are given by Fishbein et al. (1996). Temperature data at these levels are transformed into twice-daily maps using the asynoptic mapping method (Salby 1982a,b; Lait and Stanford 1988; Elson and Froidevaux 1993). Such maps are shown by Salby (1982b) to correctly resolve information gathered by the asynoptic satellite sampling. The procedure of Canziani et al. (1994) is used to organize the along-track MLS data prior to applying the method. Application of the method is given in Limpasuvan and Leovy (1995). Signals with frequencies greater than 0.8 cycle per day (period less that 1.23 days) are removed from the maps.

As this study focuses mainly on disturbances in the tropical and subtropical regions, the latitudinal data extent in the produced maps is limited to between 28° latitude in one hemisphere and 68° latitude in the opposite hemisphere during a yaw period. The spatial and temporal coverage of the analyzed data is demonstrated in Fig. 1; data areas are not covered by hatches or shadings. Three austral and two boreal summers are available for analysis. The 1994 boreal summer is not analyzed due to numerous dates with missing data in the record. In each summer season, five time periods are amenable for detailed examination of the two-day wave temperature structure in the summer hemisphere (as marked in Fig. 1 by ''AS'' and ''BS'').

Two useful diagnostics are derived from the mapped temperature field: the zonal mean zonal wind ($\overline{u}$) and the quasigeostrophic potential vorticity meridional gradient ($\overline{q}_\varphi$). Computation of the zonal mean zonal wind uses the gradient wind balance equation in log pressure coordinates as given in Andrews et al. (1987). The geopotential field from the United Kingdom Meteorological Office stratospheric analyses serves as the boundary condition at 22 hPa to facilitate the computation. Equatorial winds between 8°N and 8°S are attained by linear interpolation. The quasigeostrophic potential vorticity meridional gradient is determined from the derived zonal wind and is given in Randel (1994). Regions where $\overline{q}_\varphi$ is less than zero satisfy the necessary condition for barotropic–baroclinic instability of the basic flow (Charney and Stern 1962; Andrews et al. 1987). Barotropic instability can occur when the horizontal curvature of the mean flow is large, while baroclinic instability can occur when the vertical curvature and/or vertical shear are large. In the summer easterly jet, combined barotropic–baroclinic instability is possible (Pfister 1985).

3. Wave structure and variability

Twice-daily temperature maps during each observed austral summer (mainly January–February) and boreal

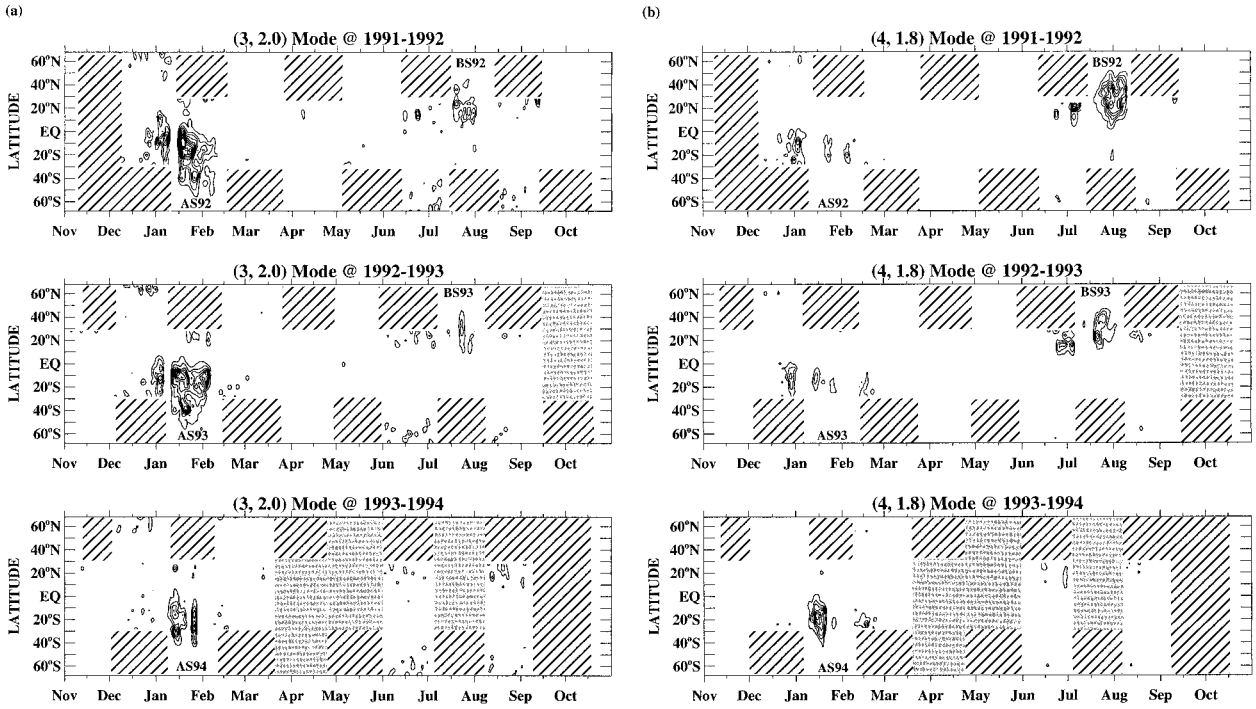

FIG. 1. (a) The (3, 2.0) mode variance at 0.46 hPa. This mode is synthesized from zonal wavenumber-3 disturbances over the westward frequency range of 0.35–0.65 cycles per day (between periods of 2.86–1.54 days). The contour interval is 1.0 K^2, starting at the 1.0 K^2 contour line. Hatched regions indicate times when no data are available and filled regions indicate times when no analysis is done (b) Same as (a) except for the (4, 1.8) mode variance at 0.46 hPa. The mode is synthesized from zonal wavenumber-4 disturbances over the westward frequency range of 0.40–0.70 cycles per day (between periods of 2.50–1.43 days).

summer (mainly July–August) show clear two-day period, westward-propagating (3, 2.0) and (4, 1.8) components around 1 hPa and above. Maps of the (3, 2.0) component are qualitatively similar to those of Rodgers and Prata (1981) who observed the wavenumber-3 two-day brightness temperature wave using measurements from the Nimbus satellites, although the (3, 2.0) amplitudes are stronger in the MLS data (not shown). The (4, 1.8) mode is less widely known. Figure 2 shows 0.46-hPa maps during the 1992 boreal summer when a strong (4, 1.8) wave event occurred. Cold anomalies are seen to concentrate near 30°N and propagate westward (clockwise) with a period slightly less than two days. A full GCM simulation of the two-day wave by Norton and Thuburn (1996) produced a similar wavenumber-4 feature in potential vorticity.

Spectral analysis is used to isolate the two-day wave signal as in Limpasuvan and Leovy (1995). As strongest amplification of the temperature disturbance is expected after the solstice, preliminary analysis is performed for five postsolstitial data segments consisting of the time when the MLS instrument is scanning mainly in the summer hemisphere (AS or BS segments in Fig. 1). For the analysis, a 28-day time series is used. The ''raw'' power spectra is defined as $0.5(a^2 + b^2)$, where a and b are the Fourier coefficients. Cross-spectral calculations were computed using the formulation of Hayashi (1971). The spectra were smoothed with a normalized Gaussian filter as in Randel (1993). The method of Blackman and Tukey (1958, p. 24) was used to evaluate the number of degrees of freedom (DOFs) of the individual spectra at each latitude. Approximately five DOFs are attained, and the corresponding 95% confidence level for the coherence squared (COH^2) is about 0.55.

In three AS data segments, strong westward-propagating spectral signals are evident in the summer hemisphere with maxima between the equator and 20°S. Examples of the spectra are shown in Limpasuvan and Leovy (1995) and Limpasuvan (1998). The (3, 2.0) component period is consistently near two days, and its signature dominates over the (4, 1.8) component during 1991–92 and 1992–93 but not during 1993–94. For the two BS data segments, the dominant westward signals correspond to the (4, 1.8) component with maximum amplitude at higher latitudes (15°–35°N) than the AS case. The mode period is consistently near 1.8 days.

Computation of the corresponding red noise (background) spectra reveals that these signals generally peak well above the 99% a priori confidence level as determined by the F statistic. In fact, wave signals confined within the period band of 1.5–2.9 days (1.4–2.5 days) for the wavenumber-3 (-4) signal are statistically significant above the 95% confidence level. To elucidate

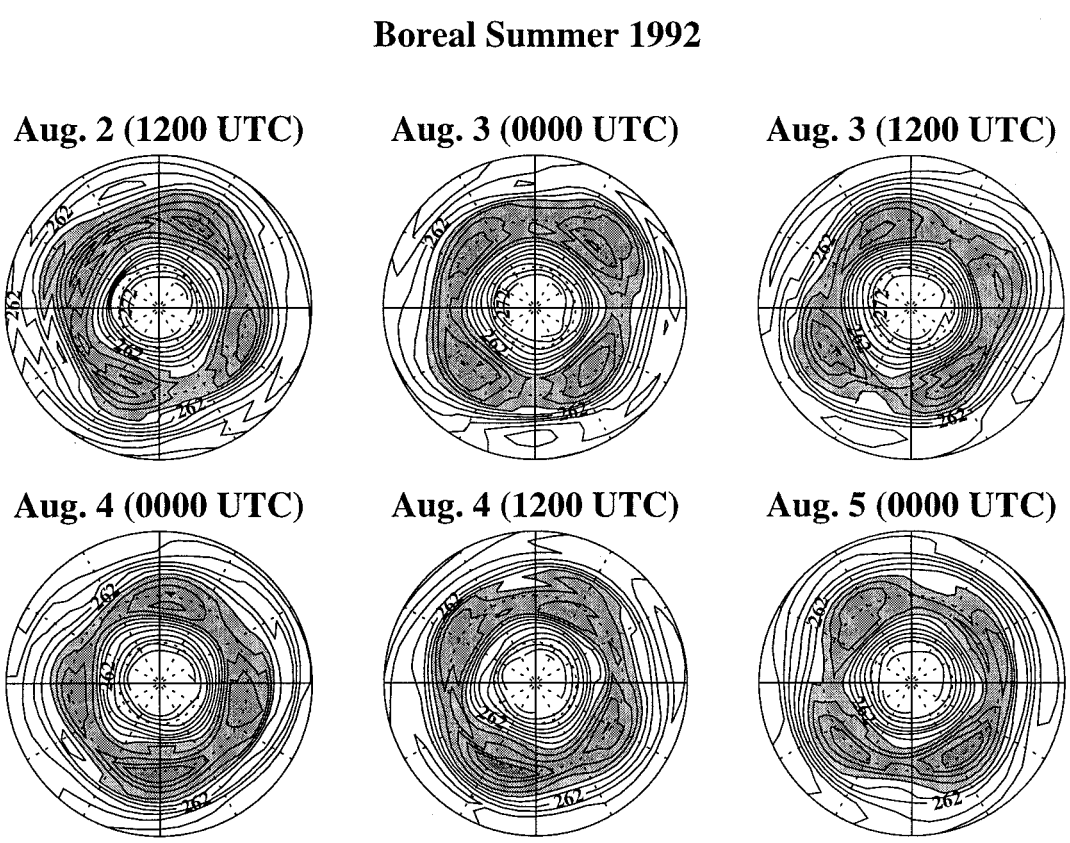

FIG. 2. Northern Hemisphere polar stereographic plots of unfiltered temperature twice-daily maps at 0.46 hPa from 1200 UTC 2 Aug 1992 to 0000 UTC 5 Aug 1992 (during data period BS92). The temperature contours are displayed every 2 K with values less than 258 K shaded. The latitude circles are in increments of 30° from the equator, and the Greenwich meridian extends directly upward from the pole.

the waves' spatial–temporal structure, a wave signal at a given wavenumber is integrated or bandpassed over these period ranges and the resulting bandpass signals are presented in subsequent figures.

Contours in Fig. 1 show the variance for the (3, 2.0) and (4, 1.8) modes at 0.46 hPa for the entire data record. The wave variance is defined as the zonal average of the squared, bandpass filtered field. The two-day wave components are observed mainly during the available AS and BS data segments when spectral analysis was done. Wave variance is confined largely to the two-month period following the solstices. The temperature disturbance predominantly resides in the summer hemisphere, although some (3, 2.0) variance is seen in the winter hemisphere.

Year-to-year variations are obvious in the time evolution of the temperature amplitudes. Intra-annually, the austral (3, 2.0) mode is at least twice as strong as the boreal (3, 2.0) mode, while the (4, 1.8) mode can be equally strong in both austral and boreal summers. The (3, 2.0) mode tends to dominate over the (4, 1.8) mode in the austral summer (except during the 1993–94 case when the amplitudes of both modes are comparable). However, during the boreal summer, the (4, 1.8) mode can have considerably larger amplitude than the (3, 2.0) mode. These patterns of modal dominance and times when the modes reach their maxima agree with the finding of Wu et al. (1996) who observed the temperature two-day wave using a different version of the 1993 MLS temperature data.

4. Background zonal flow

The top panels of Fig. 3 show the background wind evolution for each austral summer at 0.46 hPa. Easterly wind persists over much of the season in the low winter latitudes. Superimposed on this equatorial wind pattern are occasional episodes of easterly intrusion displacing the zero wind contour farther into the winter hemisphere. The austral summer easterly jet core has a magnitude of about 70–80 m s^{-1} and resides near 20°S. On the equatorward flank of the easterly core, horizontal wind shear is quite strong and, in the equatorial region, can exceed the Coriolis parameter (f). The areas where $f(f - a^{-1}\overline{u}_{\varphi}) < 0$ (here, a is the earth's radius) can be inertially unstable and are enclosed by the bold dashed line.

Six-day-averaged cross sections of the background

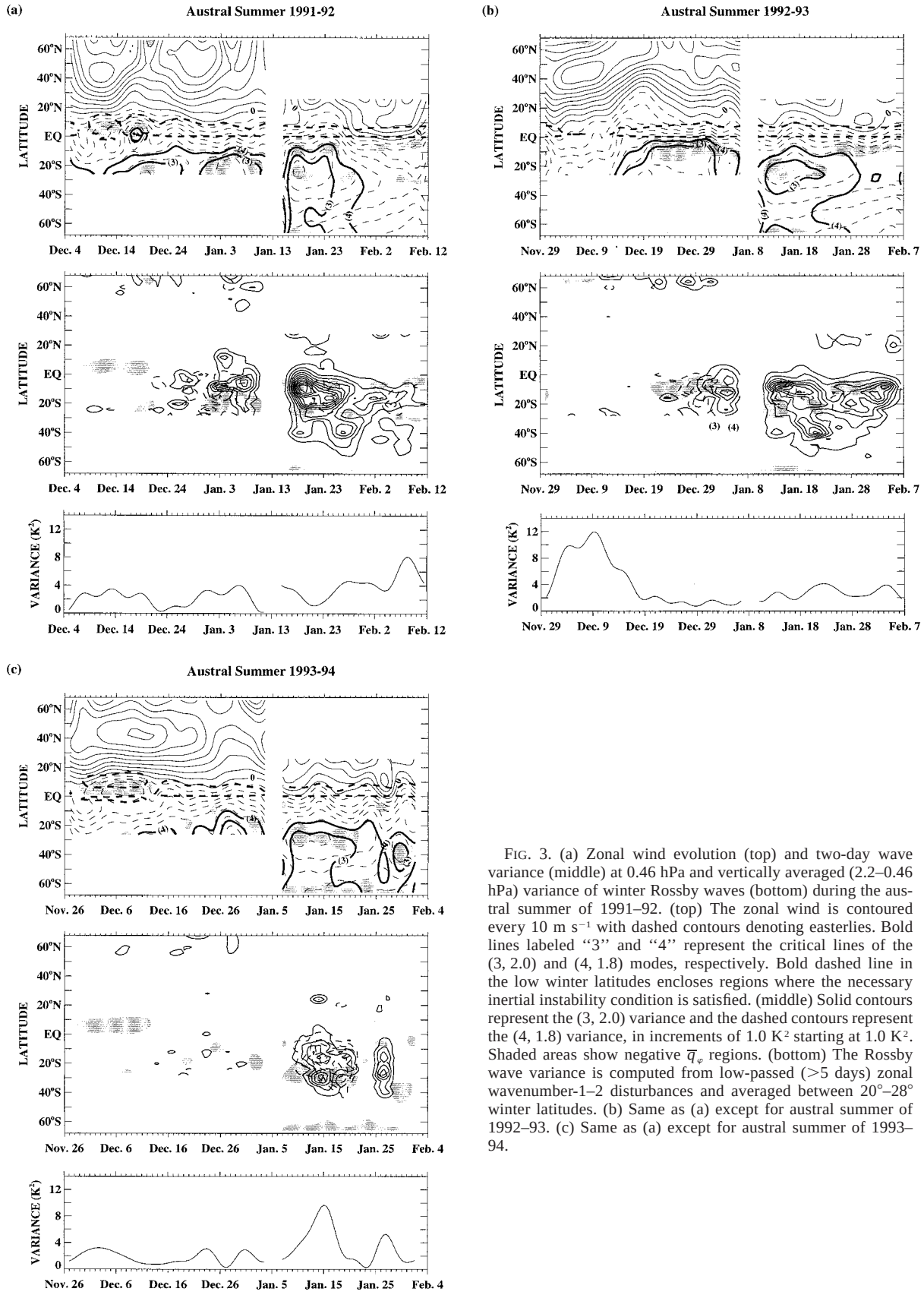

FIG. 3. (a) Zonal wind evolution (top) and two-day wave variance (middle) at 0.46 hPa and vertically averaged (2.2–0.46 hPa) variance of winter Rossby waves (bottom) during the austral summer of 1991–92. (top) The zonal wind is contoured every 10 m s^{-1} with dashed contours denoting easterlies. Bold lines labeled ''3'' and ''4'' represent the critical lines of the (3, 2.0) and (4, 1.8) modes, respectively. Bold dashed line in the low winter latitudes encloses regions where the necessary inertial instability condition is satisfied. (middle) Solid contours represent the (3, 2.0) variance and the dashed contours represent the (4, 1.8) variance, in increments of 1.0 K^2 starting at 1.0 K^2. Shaded areas show negative $\overline{q}_\varphi$ regions. (bottom) The Rossby wave variance is computed from low-passed (>5 days) zonal wavenumber-1–2 disturbances and averaged between 20°–28° winter latitudes. (b) Same as (a) except for austral summer of 1992–93. (c) Same as (a) except for austral summer of 1993–94.

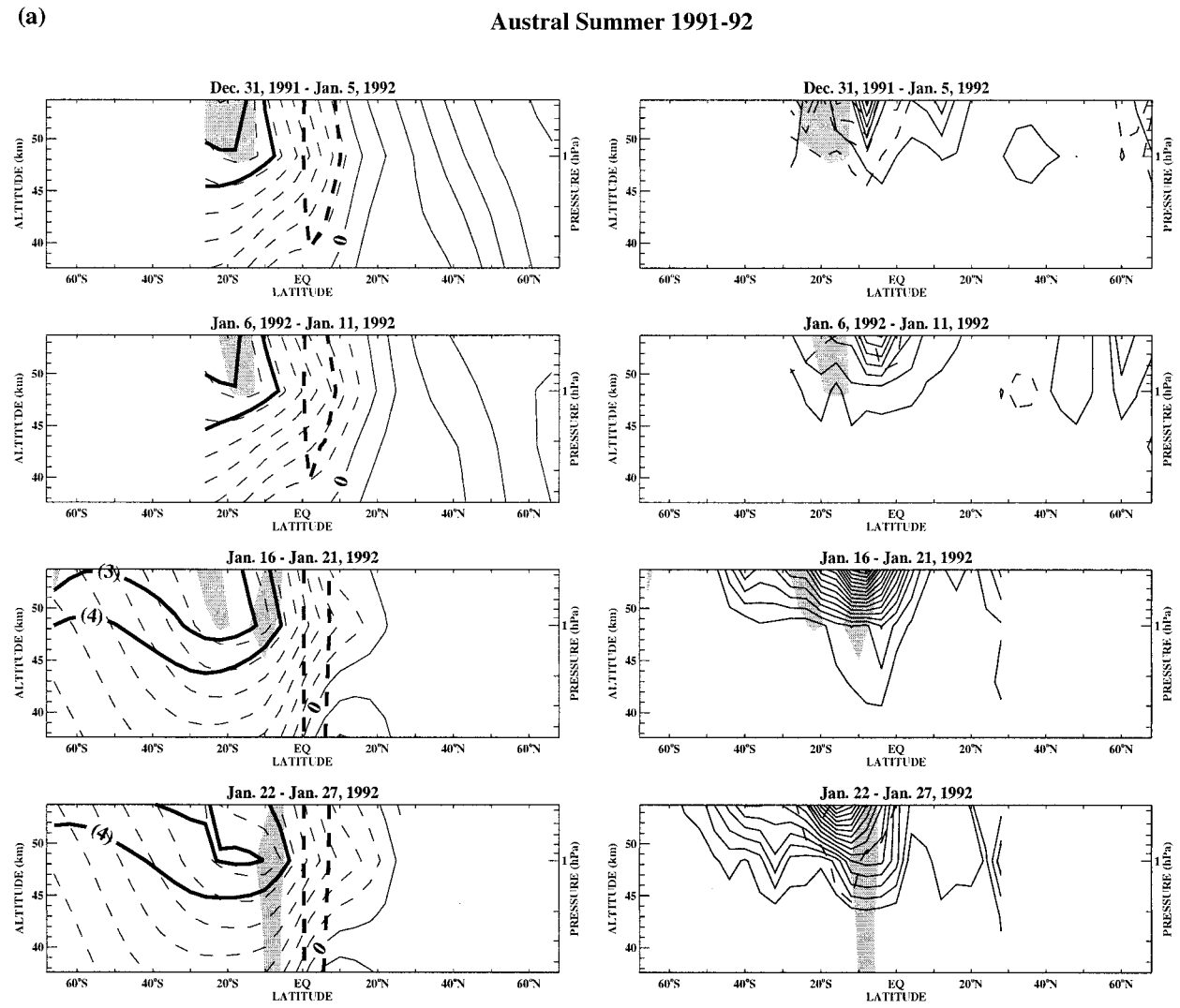

FIG. 4. (a) Six-day-averaged cross sections of the zonal mean zonal wind (left) and temperature two-day wave variance (right) for austral summer of 1992–93. The plotting convention is the same as in Fig. 3. (b) Same as (a) except for austral summer of 1992–93. (c) Same as (a) except for austral summer of 1993–94.

flow (Fig. 4, left column) show that the inertially unstable region and winterward easterly protrusion extend over great depth across the stratopause. Near the stratopause, easterly winds extend to at least 20° latitude in the winter hemisphere. Notable regions of negative $\overline{q}_{\varphi}$ (shaded) appear in low summer latitudes after the solstice (Figs. 3 and 4). These regions where the necessary condition for baroclinic–barotropic instability is satisfied are found near the easterly jet core and its equatorward flank and can also be vertically deep. In the 1993–94 case, when the wavenumber-3 component is less well developed than in the other two years, the negative $\overline{q}_{\varphi}$ regions appear to be shallowest. We caution, however, that the delineation of negative $\overline{q}_{\varphi}$ regions using temperature data of limited spatial resolution and accuracy is only approximate, especially at low latitudes.

The austral summer easterlies can potentially support critical lines of the (3, 2.0) and (4, 1.8) modes. These lines, where the waves' zonal phase speed matches the mean zonal wind, are approximated by the bold lines labeled ''3'' and ''4'' as shown in Figs. 3 and 4. For the (3, 2.0) mode, the 2.0-day period is used to determine the wave zonal phase speed; for the (4, 1.8) mode, the 1.8-day period is used. In reality, the ''actual'' critical line is only present when an unstable growing wave occurs. In this study, approximate critical lines serve only as a diagnostic tool that suggests the instability location and the background wind's ability to support the unstable modes (see sec-

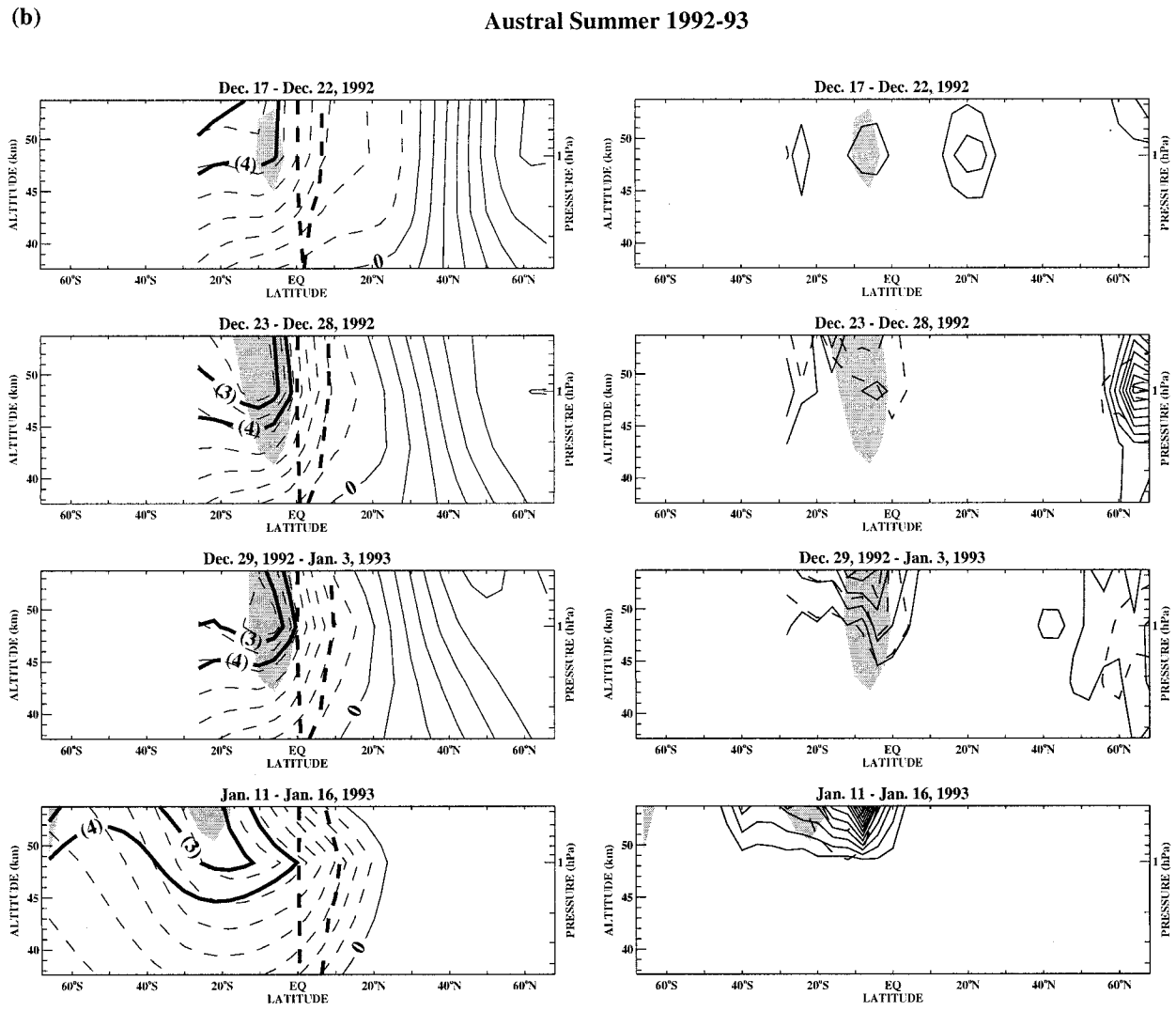

FIG. 4. *(Continued)*

tion 5). Its absence is perhaps equally important in indicating the missing instability behavior. For the austral summer easterlies, the critical lines of both modes tend to intersect or appear in close proximity to the negative $\overline{q}_\varphi$ regions.

The boreal summer easterly jet is considerably weaker and tilts more poleward with height than the austral summer easterly jet (Figs. 5 and 6 for the 1992 boreal summer). Consequently, boreal summer easterlies can potentially support only the (4, 1.8)-mode critical line within the analyzed domain. This lone critical line resides near the highest observed level where very shallow negative $\overline{q}_\varphi$ regions are found near the center of the easterly jet core. Similar to the austral summers, episodes of deep winterward easterly intrusion are observed, and the lower winter latitude region is potentially inertially unstable over much of the season. A deep negative $\overline{q}_\varphi$ region is found adjacent to the inertially unstable region. The characteristics of the 1992 boreal summer are very similar to the 1993 boreal summer case (not shown).

5. Possible mechanisms

a. Wave instability

The two-day wave variance at 0.46 hPa is presented in the middle panels of Figs. 3 and 5. The time-averaged cross sections of the variance are given in the right columns of Figs. 4 and 6. The (3, 2.0) and (4, 1.8) variances are shown in solid and dashed contours, respectively. The temperature two-day wave variances in the summer hemisphere are found on the equatorward flank and/or near the core of the easterly jet. They are also found near negative $\overline{q}_\varphi$ regions that, particularly in the austral summer, intersect or appear in close proximity

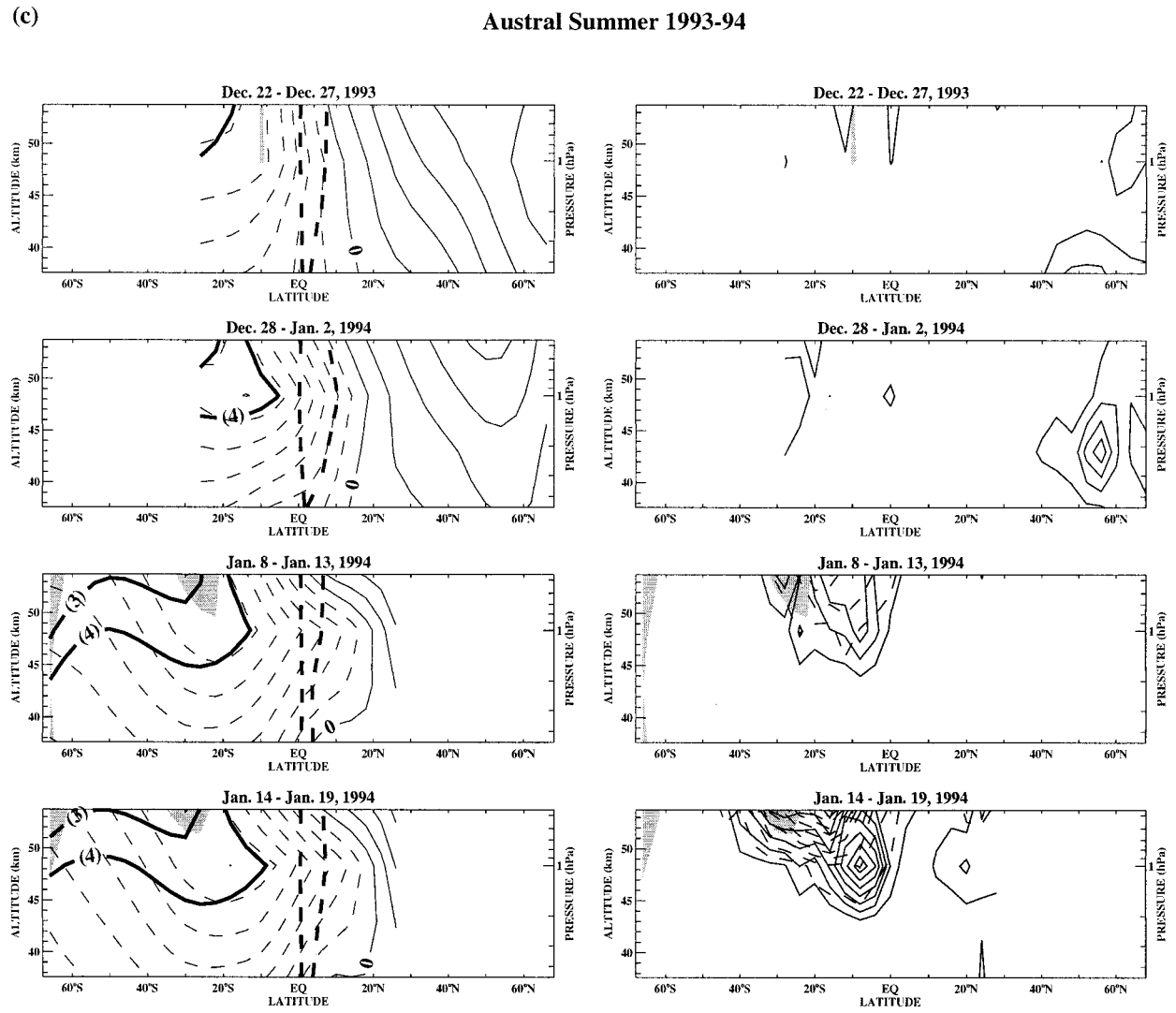

FIG. 4. *(Continued)*

to the critical lines of either or both two-day modes. On the surface, these characteristics suggest that the two-day wave is generated through instability mechanisms. Theoretically, in or near negative $\overline{q}_\varphi$ regions, the critical line acts like an unstable wave source from which Eliassen–Palm flux of the growing wave appears to emanate (Lindzen and Tung 1978; Lindzen and Barker 1985; Pfister 1987; Salby 1996). An instability interpretation of the two-day wave has been given on the basis of past observations (e.g., Burks and Leovy 1986; Randel 1994).

During the austral summers, the correspondence between the two-day wave temperature amplitude, wavenumber-3 and -4 critical lines, and regions of negative $\overline{q}_\varphi$ is best in 1992–93 and worst in 1993–94. In the latter summer, the negative $\overline{q}_\varphi$ regions appear to be confined above 50 km, and the primary seat of instability may be above the analyzed domain. Wu et al. (1996) observe downward propagation of the two-day wave temperature amplitude from 73 to about 56 km (0.46 hPa) during a similar time period.

During the 1992–93 austral summer, the development of the mean flow structure and waves strongly suggests barotropic instability as the cause for the two-day wave near the stratopause (Figs. 3b and 4b). Prior to onset of the wave signatures, easterly zonal wind contours tighten (''bunch up'') around 5°–10°S during mid- to late December, increasing the horizontal wind curvature in the low summer latitudes and contributing to the negative $\overline{q}_\varphi$ regions on the equatorward flank of the easterly jet core. As the wave amplitudes saturate (early to mid-January), the easterly jet core weakens, while equatorial easterlies strengthen. This is consistent with wave flux of westerly momentum from the equatorial region to-

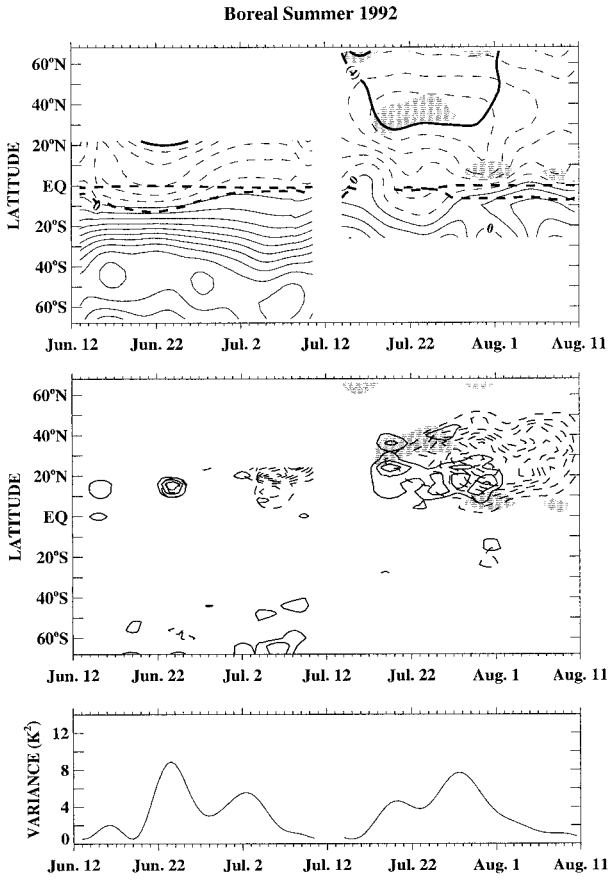

FIG. 5. Same as Fig. 3 except for boreal summer of 1992.

ward the easterly jet core, as expected for a barotropically unstable wave.

Similar tightening (albeit less intense) of the zonal mean flow contours can be seen prior to wave onset in 1991–92 and 1993–94 austral summers (Figs. 3a,c). Rapid decay of jet strength also occurs shortly after wave amplitude saturation (e.g., 24 January 1992), but the relationship between the wave amplitude evolution and weakening easterly jet is not consistent throughout this dataset.

During the boreal summers, the jet is weaker and only a wavenumber-4 critical line appears near the highest latitudes and altitudes of the domain (Figs. 5 and 6). Although a region of negative $\overline{q}_\varphi$ appears and extends as low as 45 km on the low-latitude flank of the jet, it is far removed from this critical line. However, an association between a negative $\overline{q}_\varphi$ region, a (4, 1.8) critical line, and the onset of the two-day wave amplitudes at the top of the domain (0.46 hPa) near 30°N does appear on about 18 July (Fig. 5, top panel). Thus, barotropic instability does not seem relevant. Instead, it is likely that vertical shear and curvature of the flow near the jet core, largely above the domain, excites the (4, 1.8) mode by baroclinic instability, as proposed by Norton and Thuburn (1997) and suggested by the observations of Wu et al. (1996). It is worth noting that the (4, 1.8) and (3, 2.0) amplitudes are comparable only during the 1993–94 austral summer, which is the austral summer with the weakest easterly jet, most closely resembling the typical boreal summer easterly jet.

b. Planetary Rossby waves and inertial instability

Quasi-stationary, winter Rossby waves can propagate meridionally into the equatorial regions. The bottom panels of Figs. 3 and 5 show the Rossby wave variance in the low winter latitudes. The variance is computed from zonal wavenumber-1 and -2 disturbances that have been low-pass filtered to retain only signals slower than a five-day period. The variance is then latitudinally averaged from 20° to 28° winter latitudes and vertically averaged from 2.2 to 0.464 hPa. The observed persistence of the deep protrusion of easterlies into the low winter latitudes is associated in part with the prolonged presence (and damping) of the Rossby waves throughout much of the season. Wave damping can locally affect the mean flow directly or drive a residual mean circulation that advects easterlies across the equator. Strong amplification of Rossby waves around 6 December 1992 precedes the pronounced easterly wind intrusion into the winter hemisphere around 19 December 1992 (see Figs. 3b and 4b). Another notable event occurs around 22 June 1992 (Fig. 5).

Near the stratopause, cross-equatorial advection by residual mean circulation, induced by damping of Rossby waves (and possibly also westward-propagating gravity waves) in the low winter subtropics, tends to produce strong cross-equatorial wind shear. By angular momentum conservation, the advected easterlies are strengthened as parcels move equatorward, while the advected westerlies are also strengthened as parcels move away from the equator. In regions of strong cross-equatorial shear, the normal (''usual'') gradient of angular momentum can be reversed. From the zonally symmetric point of view, a region where $f(f - a^{-1}\overline{u}_\varphi) < 0$ is said to fulfill the necessary condition for inertial instability and is shown in Figs. 3–6. Locally, this condition occurs when anomalous Ertel's potential vorticity exists (i.e., with the wrong sign in a given hemisphere), as discussed by O'Sullivan and Hitchman (1992) and Hayashi et al. (1998).

Observational evidence of inertial instability within the periods of early winter 1992 to early spring 1993 has recently been presented by Hayashi et al. (1998). They use the *UARS* Cryogenic Limb Array Etalon Spectrometer (CLAES) temperatures to elucidate the vertically stacked disturbance (''pancake'') structure associated with inertial waves (Hitchman et al. 1987). The CLAES data product has finer vertical resolution (about 2.5 km) than the MLS data, so it is amenable for the investigation of disturbances of small vertical scale (~5–14 km). Hayashi et al. show that inertial instability disturbances are readily observed in the winter sub-

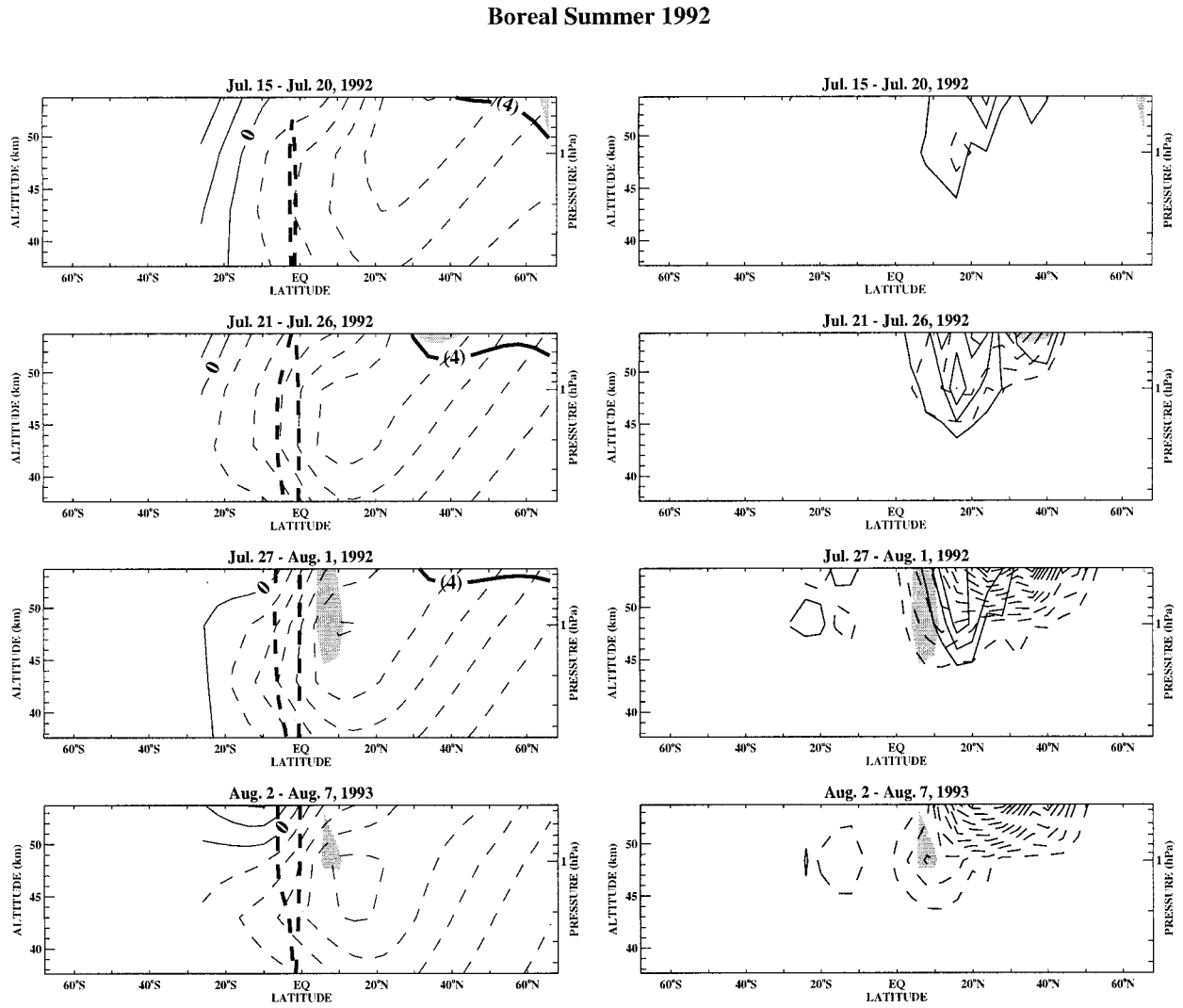

FIG. 6. Same as Fig. 4 except for boreal summer of 1992.

tropics on several occasions around each sampled solstice period. Midlatitude Rossby waves are also observed to peak nearly in coincidence with the inertial instability features suggesting that, upon propagating into the winter subtropics, Rossby waves tend to locally draw easterlies across the equator and thus initiate and organize the inertial instability structure (as noted by Hitchman et al. 1987; O'Sullivan and Hitchman 1992; Sassi et al. 1993). The relative strength and timing of the Rossby wave peaks shown in Figs. 3a,b and 5 agree quite well with the indices shown in Fig. 10 of Hayashi et al. The low-latitude Rossby wave variance during the boreal summer can be comparable to that of the austral summer.

Large variance associated with inertial instability is observed around 10–20 December 1992 (see Fig. 9 of Hayashi et al. 1998) and coincides with a deep layer of strong easterly protrusion into the winter subtropics as the winter Rossby wave is damped (17–22 December in Figs. 3b and 4b). The circulation associated with the inertial waves tends to transport westerly momentum equatorward thereby increasing the horizontal curvature near the equatorward flank of the easterly jet and contributing barotropically to its destabilization (as discussed by Hitchman 1985; Orsolini et al. 1997). The noted tightening of the equatorial easterlies and negative $\overline{q}_{\varphi}$ region after the inertial waves observed by Hayashi et al. (1998) implicate such a destabilization process and subsequent amplification of the two-day wave during the 1992–93 austral summer. Hence, overlapping CLAES and MLS observations support a possible connection among midlatitude winter Rossby waves, inertial waves, and the two-day waves during the 1992–93 austral summer.

Any possible link between inertial instability and the two-day wave during other austral or boreal summers is not so straightforward. In Hayashi et al. (1998), observed inertial waves during the 1991–92 austral sum-

mer are only partially covered in the CLAES record, while data beyond June 1993 were not analyzed. However, inertial waves are reported during late January 1992 and late July and early August 1992 (see their Fig. 9) when deep negative $\overline{q}_\varphi$ regions appear on the equatorward flank of the easterly jet (Fig. 4a, last two rows and Fig. 6, third row). In early August 1992, a preceding strong Rossby wave signature in the low winter subtropics that may have initiated inertial waves is also evident in Fig. 5 (bottom).

c. Normal mode and precursory winter signal

Relatively weak two-day wave variance is found in the low winter latitudes (e.g., Fig. 4, right columns, and in Fig. 6 of Wu et al. 1996). As discussed in Salby (1981), the Rossby normal mode amplitude appears most amplified near regions where the zonal wind is slightly smaller than its phase speed (i.e., small Doppler-shifted frequency), near the core of the easterly jet. The vertical evanescence of the normal mode amplitude is greatly reduced in these regions. Indeed, the observed (3, 2.0) mode is consistently found near small Doppler-shifted frequency regions during both summers. These features suggest normal-mode-like characteristics in the observed two-day wave especially during the boreal summers when weak (3, 2.0) variance is observed in the absence of a (3, 2.0) critical line within the observational domain. Mixed wave instability and normal mode characteristics have been discussed by various authors (e.g., Burks and Leovy 1986; Randel 1994; Wu et al. 1996).

Bursts of (3, 2.0) variance can also be found at high winter latitudes in each austral summer in association with broad spectrum amplification of transient planetary waves. During the 1992–93 austral summer, particularly strong winter (3, 2.0) variance is observed near 1 hPa and poleward of 60°N (see Fig. 4b, right). During other austral summers, weaker winter (3, 2.0) variance is found at lower levels (e.g., Fig. 4c). The winter (3, 2.0) signal appears about a week prior to the appearance of strong two-day wave variance at low summer latitudes. A precursory (3, 2.0) winter signal was noted by Wu et al. (1996) during the 1992–93 austral summer, and the meridional structure presented in Fig. 4b is in good agreement with their results. Wu et al. suggest that the initial winter signal may trigger the summer two-day wave as it penetrates (leaks) into the summer hemisphere. This forcing then becomes enhanced in the unstable region above the easterly jet core due to matched frequency and wavenumber between the signal propagating from winter high latitudes and the unstable modes. Our analysis suggests that this mechanism is possible during each austral summer.

6. Summary

The 3-yr *UARS* MLS temperature dataset (December 1991–September 1994) provides considerable insight into the behavior of the two-day wave near the stratopause. Current findings reveal not only the variable nature of this recurrent phenomenon but also clues about its complex origin. In agreement with previous satellite observations (viz., Rodgers and Prata 1981; Burks and Leovy 1986; Wu et al. 1996), two components of the two-day wave are discovered, corresponding to zonal wavenumbers 3 and 4 with 2-day and 1.8-day periods, respectively. Evidence of the two-day wave is readily seen in twice-daily maps of the temperature field near the highest observed levels (1.0–0.46 hPa).

Intra-annually, the (3, 2.0) component during the austral summer is nearly twice as strong as its boreal summer counterpart. The (4, 1.8) component, on the other hand, can be equally strong in both summers. In comparing their relative magnitudes, the (3, 2.0) component tends to be larger and of longer duration than (4, 1.8) during the austral summer. An exception occurs during the 1993–94 austral summer when both modes appear equally pronounced. Observations from Limb Infrared Monitor of the Stratosphere data for the 1978–79 austral summer by Burks and Leovy (1986) also found both two-day wave components to be equally strong. While the cause of interannual variability of the relative temperature amplitudes of these modes is uncertain, comparisons between three austral summers point to the role of variations in easterly jet strength (weaker jets favor wavenumber-4 mode and conversely). Interannual variations in the easterly jet strength can, in turn, be traced back to interannual variations in winter Rossby wave forcing (Ray et al. 1998).

Prevailing processes like gravity wave breaking and inertial instability can continually destabilize the summer easterly jet. Gravity wave drag on the mean flow can baroclinically destabilize the easterly jet near the core (as noted by Plumb 1983; Norton and Thuburn 1996, 1997), while inertial instability adjustment can barotropically destabilize the equatorward flank of the easterly jet. Joint effects of these processes can make instability interpretation of the two-day wave difficult as potentially unstable regions of reversed mean potential vorticity gradient (negative $\overline{q}_\varphi$) can intermittently appear throughout the season in the 40–58-km layer analyzed here.

Barotropic instability interpretation of wave generation during the austral summers is based on the joint occurrence of negative $\overline{q}_\varphi$ regions, wavenumber-3 and -4 critical lines, and wavenumber-3 and -4 temperature amplification near the equatorward flank of the easterly jet. During the 1992–93 austral summer, the jet weakens as the wave amplitude saturates, as expected for wave–mean flow interaction in a barotropically unstable regime. However, this behavior is not consistently observed. During the 1993–94 austral summer, the seat of the instability may be above our observational domain. Boreal summer amplification of the (4, 1.8) component is likely to arise from instability above the altitude range of our observations and may be due to baroclinic in-

stability, as suggested by Norton and Thuburn (1996, 1997).

Barotropic instability and the associated two-day wave during the austral summers appear to be linked to inertial instability disturbances organized by Rossby waves in the low winter latitudes. Concurrent inertial waves and winter Rossby wave signatures are reported by Hayashi et al. (1998) using the *UARS* CLAES temperature data at times when negative $\overline{q}_\varphi$ regions associated with strong meridional curvature of the easterly jet appear in our analysis.

These results do not preclude a role of Rossby normal mode amplification of (3, 2.0) near the easterly jet, especially during the boreal summers. Consistent with the normal mode interpretation, meridional structures do show amplification of the (3, 2.0) temperature wave amplitude in low winter latitudes that is nearly out of phase with the low summer latitude signature during its peak (Limpasuvan and Leovy 1995). However, the winter temperature peak is relatively weak and can be sporadic suggesting that, if it is a normal mode, it is strongly dissipated.

Like Wu et al. (1996), we find precursory two-day wave signals in the high winter latitudes (poleward of 50°) before the strong two-day wave episodes in the summer hemisphere. Thus, our analysis does not rule out the hypothesis of Wu et al. that the high winter latitude wave triggers the two-day wave in the summer hemisphere as it leaks across the equator.

Acknowledgments. We thank the *UARS* MLS science team for the dataset and Dr. Pablo O. Canziani for the computer code used to arrange the data into format suitable for the asynoptic method. We also thank three anonymous reviewers who helped improve the manuscript significantly and appreciate Mr. Hiroo Hayashi for providing us with a preliminary draft of the Hayashi et al. (1998) paper during the preparation of our manuscript. This work was supported by NASA under Grant NAG5-3188 and is based in part on VL's Ph.D. dissertation at the University of Washington.

REFERENCES

Andrews, D. G., J. R. Holton, and C. B. Leovy, 1987: *Middle Atmospheric Dynamics.* Academic Press, 489 pp.

Barath, F. T., and Coauthors, 1993: The *Upper Atmosphere Research Satellite* Microwave Limb Sounder instrument. *J. Geophys. Res.,* **98,** 10 751–10 762.

Blackman, R. B., and J. W. Tukey, 1958: *The Measurement of Power Spectra.* Dover Press, 190 pp.

Burks, D., and C. B. Leovy, 1986: Planetary waves near the mesospheric easterly jet. *Geophys. Res. Lett.,* **13,** 193–196.

Canziani, P. O., J. R. Holton, E. F. Fishbein, L. Froidevaux, and J. W. Waters, 1994: Equatorial Kelvin waves: A *UARS* MLS view. *J. Atmos. Sci.,* **51,** 3053–3076.

Charney, J. G., and M. E. Stern, 1962: On the stability of internal baroclinic jets in a rotating atmosphere. *J. Atmos. Sci.,* **19,** 159–172.

Elson, L. S., and L. Froidevaux, 1993: Use of Fourier transforms for asynoptic mapping: Applications to the *Upper Atmosphere Research Satellite* Microwave Limb Sounder. *J. Geophys. Res.,* **98,** 23 039–23 049.

Fishbein, E. F., and Coauthors, 1996: Validation of *UARS* Microwave Limb Sounder temperature and pressure measurements. *J. Geophys. Res.,* **101,** 9983–10 016.

Fritts, D. C., L. Yuan, M. H. Hitchman, L. Coy, E. Kudeki, and R. F. Woodman, 1992: Dynamics of the equatorial mesosphere observed using the Jicamarca MST radar during June and August 1987. *J. Atmos. Sci.,* **49,** 2353–2371.

Hayashi, H., M. Shiotani, and J. C. Gille, 1998: Vertically stacked temperature disturbances near the equatorial stratopause as seen in cryogenic limb array etalon spectrometer data. *J. Geophys. Res.,* **103,** 19 469–19 483.

Hayashi, Y., 1971: A generalized method of resolving disturbance into progressive and retrogressive waves by space Fourier and time cross-spectral analyses. *J. Meteor. Soc. Japan,* **49,** 125–128.

Hitchman, M. H., 1985: An observational study of wave-mean flow interaction in the equatorial middle atmosphere. Ph.D. dissertation, Department of Atmospheric Sciences, University of Washington, 360 pp. [Available from Dept. of Atmospheric Sciences, University of Washington, Box 351640, Seattle, WA 98195.]

——, C. B. Leovy, J. C. Gille, and P. L. Bailey, 1987: Quasi-stationary zonally asymmetric circulations in the equatorial lower mesosphere. *J. Atmos. Sci.,* **44,** 2219–2236.

Lait, L. R., and J. L. Stanford, 1988: Applications of asynoptic space–time Fourier transform methods to scanning satellite measurements. *J. Atmos. Sci.,* **45,** 3784–3799.

Limpasuvan, V., 1998: Tropical dynamics near the stratopause: The two-day wave and its relatives. Ph.D. dissertation, Department of Atmospheric Sciences, University of Washington, 209 pp. [Available from Dept. of Atmospheric Sciences, University of Washington, Box 351640, Seattle, WA 98195.]

——, and C. B. Leovy, 1995: Observation of the two-day wave near the southern summer stratopause. *Geophys. Res. Lett.,* **22,** 2385–2388.

Lindzen, R. S., and K. K. Tung, 1978: Wave overreflection and shear instability. *J. Atmos. Sci.,* **35,** 1626–1632.

——, and J. W. Barker, 1985: Instability and wave over-reflection in stably stratified shear flow. *J. Fluid Mech.,* **151,** 189–217.

Muller, H. G., and L. Nelson, 1978: A traveling quasi 2-day wave in the meteor region. *J. Atmos. Terr. Phys.,* **40,** 761–766.

Norton, W. A., and J. Thuburn, 1996: The two-day wave in a middle atmosphere GCM. *Geophys. Res. Lett.,* **23,** 2113–2116.

——, and ——, 1997: The mesosphere in the extended UGAMP GCM. *Gravity Wave Processes and Their Parametrization in Global Climate Models,* K. Hamilton, Ed., Vol. 50, Springer-Verlag, 383–401.

Orsolini, Y. J., V. Limpasuvan, and C. B. Leovy, 1997: The tropical stratopause in the UKMO assimilated analyses: Evidence for a 2-day wave and inertial circulations. *Quart. J. Roy. Meteor. Soc.,* **123,** 1707–1724.

O'Sullivan, D. J., and M. H. Hitchman, 1992: Inertial instability and Rossby wave breaking in a numerical model. *J. Atmos. Sci.,* **49,** 991–1002.

Pfister, L., 1985: Baroclinic instability of easterly jets with applications to the summer mesosphere. *J. Atmos. Sci.,* **42,** 313–330.

Plumb, R. A., 1983: Baroclinic instability at the summer mesosphere: A mechanism for the quasi-two-day wave? *J. Atmos. Sci.,* **40,** 262–270.

Randel, W. J., 1993: Global normal-mode Rossby waves observed in stratospheric ozone data. *J. Atmos. Sci.,* **50,** 406–420.

——, 1994: Observations of the 2-day wave in NMC stratospheric analyses. *J. Atmos. Sci.,* **51,** 306–313.

Ray, E. A., M. J. Alexander, and J. R. Holton, 1998: An analysis of the structure and forcing of the equatorial semiannual oscillation in zonal wind. *J. Geophys. Res.,* **103,** 1759–1774.

Rodgers, C. D., and A. J. Prata, 1981: Evidence for a traveling 2-day wave in the middle atmosphere. *J. Geophys. Res.*, **86,** 9661–9664.

Salby, M. L., 1981: The 2-day wave in the middle atmosphere: Observations and theory. *J. Geophys. Res.*, **86,** 9654–9660.

——, 1982a: Sampling theory for asynoptic satellite observations. Part I: Space–time spectra, resolution, and aliasing. *J. Atmos. Sci.*, **39,** 2577–2600.

——, 1982b: Sampling theory for asynoptic satellite observations. Part II: Fast Fourier synoptic mapping. *J. Atmos. Sci.*, **39,** 2601–2614.

——, 1996: *Fundamentals of Atmospheric Physics.* Academic Press, 627 pp.

Sassi, F., R. R. Garcia, and B. A. Boville, 1993: The stratopause semiannual oscillation in the NCAR community climate model. *J. Atmos. Sci.*, **50,** 3608–3624.

Vincent, R. A., 1984: MF/HF radar measurements of the dynamics of the mesopause region—A review. *J. Atmos. Terr. Phys.*, **11,** 961–974.

Wu, D. L., E. F. Fishbein, W. G. Read, and J. W. Waters, 1996: Excitation and evolution of the quasi-2-day wave observed in *UARS*/MLS temperature measurements. *J. Atmos. Sci.*, **53,** 728–738.